A Simple Sensorless Scheme for Induction Motor Drives Fed by a Matrix Converter Using Constant Air-Gap Flux and PQR Transformation

Kyo-Beum Lee and Frede Blaabjerg

Abstract: This paper presents a new and simple method for sensorless operation of matrix converter drives using a constant air-gap flux and the imaginary power flowing to the motor. To improve low-speed sensorless performance, the non-linearities of a matrix converter drive such as commutation delays, turn-on and turn-off times of switching devices, and on-state switching device voltage drop are modeled using PQR transformation and compensated using a reference current control scheme. The proposed compensation method is applied for high performance induction motor drives using a 3 kW matrix converter system. Experimental results are shown to illustrate the feasibility of the proposed strategy.

Keywords: Non-linearity compensation, PQR power transformation, sensorless matrix converter drive.

1. INTRODUCTION

Induction motor drives fed by a matrix converter have been developed for the last decades [1]. The matrix converter drive has recently attracted the industry application and the technical development has been further accelerated because of increasing importance of power quality and energy efficiency issues. The induction motor drive fed by matrix converter is superior to the conventional inverter because of the lack of the bulky DC-link capacitors with limited life time, the bi-directional power flow capability, the sinusoidal input/output currents, and adjustable input power factor. Furthermore, because of the high integration capability and the higher reliability of the semiconductor structures, the matrix converter topology is recommended for extreme temperatures and critical volume/weight applications. However, a few of the practical matrix converters have been applied to induction motor drive system because the implementation of switch devices in the matrix converter is difficult. Also modulation technique and commutation control are more complicated than the conventional PWM inverter [1-8].

Adjustable speed drives are widespread electro-mechanical systems suitable for a large spectrum of industrial applications. When a high dynamic performance and precision control are required for an induction motor in a wide speed range, the speed must normally be measured. In contrast, in the case of medium and low performance applications, sensorless control without measuring the motor speed is desirable. As a consequence of this, a great deal of research has been carried out in sensorless drives over the last few decades. The advantages of speed sensorless induction motor drives are reduced hardware complexity and lower cost, reduced size of the drive machine, elimination of the sensor cable, better noise immunity, increased reliability, and less maintenance requirements. Operation in hostile environments mostly requires a motor without speed sensor [9].

In order to build a high-performance speed-sensorless control algorithm for the induction motor drives fed by a matrix converter, more accurate information on the motor speed and more robustness against motor parameters are required. In particular, in the low-speed operation, the machine model-based observer does not produce fairly satisfactory performance without a parameter adaptation scheme when the motor parameters vary in operation. Since the fundamental output voltage cannot be detected directly from the matrix converter output terminal in a matrix converter drive, the calculated average voltage is normally used instead of the actual one. However, the calculated average voltage does not agree with the actual fundamental output voltage due to non-linear characteristic of the matrix converter, such as commutation delay, turn-on and turn-off time of switching device, and on-state switching devices voltage drop. In order to compensate this problem,

Manuscript received September 6, 2006; accepted June 25, 2007. Recommended by Editor Tae-Woong Yoon.

Kyo-Beum Lee is with the School of Electrical and Computer Engineering, Ajou University, San 5, Woncheon-dong Yeongtong-gu, Suwon 443-749, Korea (e-mail: kyl@ajou.ac.kr).

Frede Blaabjerg is with the Institute of Energy Technology, Aalborg University, DK-9220 Aalborg East, Denmark (e-mail: fbl@iet.aau.dk).

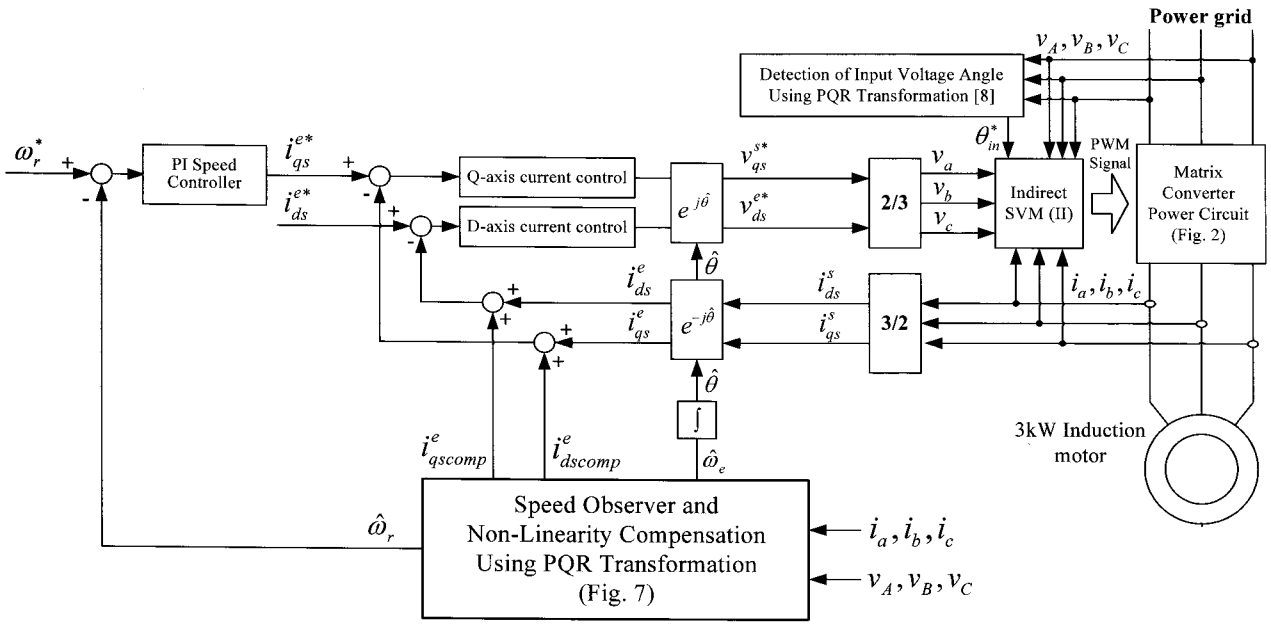

Fig. 1. The proposed sensorless vector control for matrix converter drives.

specially important at low speed, the authors have made an attempt to compensate the non-linear matrix converter effects with current sign and off-line manners [6,7]. However, it is difficult to determine the current sign when the phase currents are close to zero. If the current sign is misjudged, the non-linearity model of a matrix converter operates improperly. It is also difficult to compensate the non-linearity effects perfectly by off-line manners because the switching times and voltage drops of the power devices are varied with the operating conditions [8,10].

In this paper, a new sensorless method for matrix converter drives using a PQR power theory is proposed. Fig. 1 shows the whole control block diagram of a vector controlled matrix converter drive. The proposed technique detects the speed of the rotor of an induction motor using the constant air-gap flux and the imaginary power flowing to the motor. The paper calculates the non-linearity of matrix converter drives using the PQR transformation, and the reference current control method applies to make the compensation currents in order to improve speed sensorless operation in the low speed region. Experimental results derived from a test drive system are presented to show the performance of the proposed observer.

2. CONTROL OF A MATRIX CONVERTER DRIVE

The main circuit of a matrix converter is shown in Fig. 2. It consists of the input filter, the bi-directional power switches connected into a three-phase to three-phase matrix and a clamp circuit. The input LC filter is a second order low-pass topology, which is used to reduce the high-frequency ripple from the input current. The clamp circuit consists of two diode bridges to connect the input and the output to a clamp capacitor, in order to protect the switches against possible over-voltages that appear during transient.

The one of the possible modulation method for matrix converter is the Indirect Space Vector Modulation (ISVM) [1,2], which considers the matrix converter as a two stage transformation converter: a rectification stage to provide a constant imaginary DC-link voltage per switching period and an inverter stage to produce the three output voltages.

The input current vector, Iin that corresponds to the rectification stage and the output voltage vector, Uout that corresponds to the inversion stage are the reference vectors (Fig. 3). The indirect space vector modulation uses a combination of the two adjacent vectors and a zero vector to produce the reference vector. The ratio between the duty cycles of two

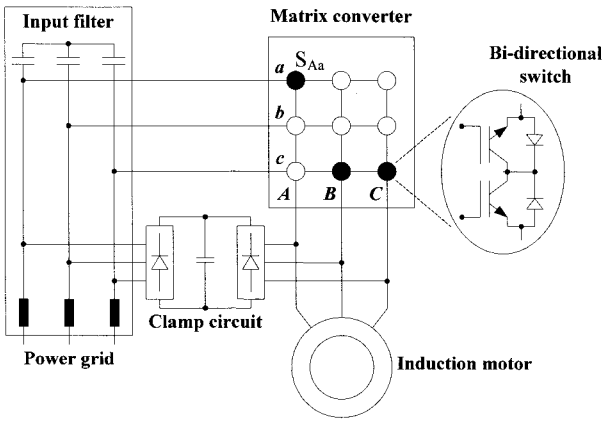

Fig. 2. The topology of a matrix converter drive.

adjacent vectors determines the direction of the reference vector.

The duty cycles of the active switching vectors for the rectification stage are calculated with (1) and the duty cycle of the active switching vectors for the inversion stage are calculated with (2).

$$d_\gamma = m_I \sin\left(\frac{\pi}{3} - \theta_{in}^*\right) \text{ and } d_\delta = m_I \sin\theta_{in}^*, \quad (1)$$

$$d_\alpha = m_U \sin\left(\frac{\pi}{3} - \theta_{out}^*\right) \text{ and } d_\beta = m_U \sin\theta_{out}^*, \quad (2)$$

where m_I and m_u are the rectification and inversion stage indexes, θ_{in}^* and θ_{out}^* inversion stage indexes, are the angles within their respective sectors of the input current and output voltage reference vectors (see Fig. 3). The input current reference vector is synthesized by impressing adjacent switching vectors, I_γ and I_δ with duty cycle d_γ and d_δ to the rectifying stage. The reference voltage vector is modulated by the impressed adjacent voltage vectors, U_α and U_β with duty-cycle d_α and d_β.

To obtain a correct balance of the input currents and the output voltages in the same switching period, the modulation pattern should produce all combinations of the rectification $(\gamma - \delta - 0)$ and the inversion $(\alpha - \beta - 0)$ switching states, resulting in the following switching pattern: $\alpha\gamma - \alpha\delta - \beta\delta - \beta\gamma - 0$.

Therefore, each duty cycle sequence is a result of the cross products of the rectification and the inversion stage duty cycles, while the duration of the zero-vector is completing the switching sequence as

$$\begin{aligned} &d_{\alpha\gamma} = d_\alpha d_\gamma, \quad d_{\alpha\delta} = d_\alpha d_\delta, \\ &d_{\beta\delta} = d_\beta d_\delta, \quad d_{\beta\gamma} = d_\beta d_\gamma, \\ &d_0 = 1 - \left(d_{\alpha\gamma} + d_{\alpha\delta} + d_{\beta\delta} + d_{\beta\gamma}\right). \end{aligned} \quad (3)$$

The duration of each sequence is found by multiplying the corresponding duty cycle to the switching period.

Normally, the matrix converter is fed by a voltage source converter and, for this reason, the input terminal should not be shorted directly. On the other hand, the load has typically an inductive nature and, for this reason, an output phase must never be opened.

Defining the switching function of a single switch as

$$S_{jk} = \begin{cases} 1, & \text{switch } S_{jk} \text{ closed} \\ 0, & \text{switch } S_{jk} \text{ open,} \end{cases} \quad (4)$$

where k={a, b, c} is input phase and j={A, B, C} is output phase.

The low-frequency transfer of the matrix converter is defined by

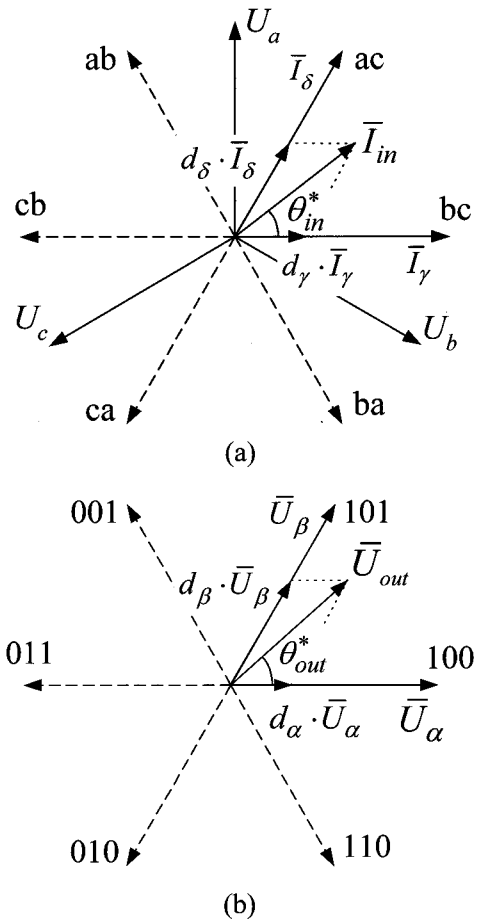

Fig. 3. Generation of the reference voltage vectors using ISVM (a) in the rectification stage, (b) in the inversion stage.

$$\mathbf{M}(t) = \begin{bmatrix} m_{Aa}(t) & m_{Ab}(t) & m_{Ac}(t) \\ m_{Ba}(t) & m_{Bb}(t) & m_{Bc}(t) \\ m_{Ca}(t) & m_{Cb}(t) & m_{Cc}(t) \end{bmatrix}. \quad (5)$$

The low-frequency component of the output phase voltage v_o is given by

$$\mathbf{v}_o(t) = \mathbf{M}(t) \cdot \mathbf{v}_i(t), \quad (6)$$

where $\mathbf{v}_0$ is the output voltage vector and $\mathbf{v}_i$ is the input voltage vector.

The low-frequency component of the input current $\mathbf{i}_i$ is

$$\mathbf{i}_i(t) = \mathbf{M}(t)^T \cdot \mathbf{i}_o(t), \quad (7)$$

where $\mathbf{i}_i$ is the input current vector and $\mathbf{i}_o$ is the output current vector.

The constraints discussed above can be expressed by

$$S_{ja} + S_{jb} + S_{jc} = 1. \quad (8)$$

With these restrictions, a 3×3 matrix converter has 27 possible switching states.

Let $m_{jk}(t)$ be the duty cycle of switch S_{jk}, defined as

$$m_{jk}(t) = t_{jk} / t_{sp}, \quad \text{where} \quad 0 < m_{jk} < 1. \tag{9}$$

3. CONSTANT AIR-GAP FLUX AND PQR TRANSFORMATION

3.1. Constant air-gap flux operation

An induction motor can be described by the following voltage equations. The corresponding equivalent circuit in the rotating d-q reference frame is shown in Fig. 4 [11].

$$\begin{aligned} v_{ds}^e &= R_s i_{ds}^e + \frac{d}{dt}\lambda_{ds}^e - \omega_e \lambda_{qs}^e, \\ v_{qs}^e &= R_s i_{qs}^e + \frac{d}{dt}\lambda_{qs}^e + \omega_e \lambda_{ds}^e, \\ 0 &= R_r i_{dr}^e + \frac{d}{dt}\lambda_{dr}^e - (\omega_e - \omega_r)\lambda_{qr}^e, \\ 0 &= R_r i_{qr}^e + \frac{d}{dt}\lambda_{qr}^e + (\omega_e - \omega_r)\lambda_{dr}^e, \end{aligned} \tag{10}$$

where the superscript 'e' is the rotating d-q reference frame, v_{ds}^e and v_{qs}^e are the stator d- and q- axis voltages, i_{ds}^e and i_{qs}^e are the stator d- and q- axis currents, i_{dr}^e and i_{qr}^e are the rotor d- and q- axis currents, λ_{ds}^e and λ_{qs}^e are the d- and q- axis stator fluxes, λ_{dr}^e and λ_{qr}^e are the d- and q- axis rotor fluxes, R_s is the stator resistance, R_r is the rotor resistance, ω_e is the synchronous angular frequency and ω_r is the rotor angular frequency.

The flux equations are given as

$$\begin{aligned} \lambda_{ds}^e &= \lambda_{dm}^e + L_{ls} i_{ds}^e, \\ \lambda_{qs}^e &= \lambda_{qm}^e + L_{ls} i_{qs}^e, \end{aligned} \tag{11}$$

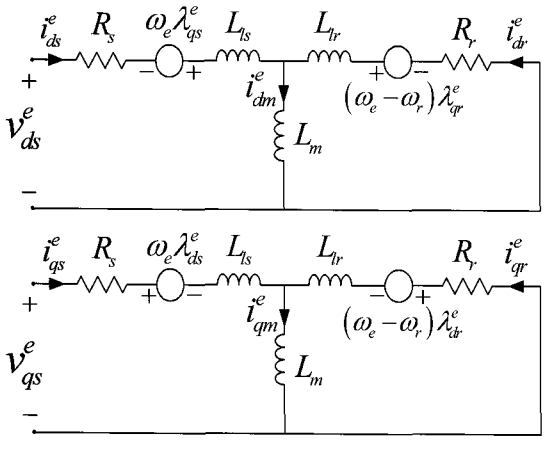

Fig. 4. d-q equivalent circuit of an induction motor.

$$\begin{aligned} \lambda_{dr}^e &= \lambda_{dm}^e + L_{lr} i_{dr}^e, \\ \lambda_{qr}^e &= \lambda_{qm}^e + L_{lr} i_{qr}^e, \\ \lambda_{dm}^e &= L_m\left(i_{ds}^e + i_{dr}^e\right) = L_m i_{dm}^e, \\ \lambda_{qm}^e &= L_m\left(i_{ds}^e + i_{dr}^e\right) = L_m i_{qm}^e, \end{aligned}$$

where λ_{dm}^e and λ_{qm}^e are the d- and q- axes air-gap fluxes, i_{dm}^e and i_{qm}^e are the d- and q- axis magnetizing currents, L_{ls} and L_{lr} are the stator and rotor leakage inductances, and L_m is the magnetizing inductance.

The stator voltage equation in (10) can be rewritten using (11) as

$$\begin{aligned} v_{ds}^e &= R_s i_{ds}^e + \frac{d}{dt}(\lambda_{dm}^e + L_{ls} i_{ds}^e) - \omega_e(\lambda_{qm}^e + L_{ls} i_{qs}^e), \\ v_{qs}^e &= R_s i_{qs}^e + \frac{d}{dt}(\lambda_{qm}^e + L_{ls} i_{qs}^e) - \omega_e(\lambda_{dm}^e + L_{ls} i_{ds}^e). \end{aligned} \tag{12}$$

If the vector control is fulfilled such that the time derivative of d- and q- axis stator currents in the rotating frame can be zero during a control sampling period, (12) can be rewritten as

$$\begin{aligned} v_{ds}^e &= R_s i_{ds}^e + \frac{d}{dt}\lambda_{dm}^e - \omega_e(\lambda_{qm}^e + L_{ls} i_{qs}^e), \\ v_{qs}^e &= R_s i_{qs}^e + \frac{d}{dt}\lambda_{qm}^e - \omega_e(\lambda_{dm}^e + L_{ls} i_{ds}^e). \end{aligned} \tag{13}$$

Ignoring the terms related to the rate of change of the air-gap fluxes λ_{dm}^e and λ_{qm}^e, (13) can be rearranged as

$$\begin{aligned} v_{ds}^e &= R_s i_{ds}^e - \omega_e(\lambda_{qm}^e + L_{ls} i_{qs}^e), \\ v_{qs}^e &= R_s i_{qs}^e + \omega_e(\lambda_{dm}^e + L_{ls} i_{ds}^e). \end{aligned} \tag{14}$$

If the voltage drop across the stator leakage impedance is negligible in comparison with $|\lambda_m|\omega_e \gg |(R_s + j\omega_e L_{ls})\mathbf{i}_s|$, then

$$|v_s| \approx |v_{emf}| \approx |\lambda_m|\omega_e = L_m |i_m|\omega_e, \tag{15}$$

where v_{emf} is the magnitude of the back- emf voltage, i_m can be inferred from the set point for the machine flux assuming that $i_m \approx \lambda_{ref}/L_m$, and under the assumption that this set point is being achieved by the controller.

The magnitude of magnetizing current $|i_m|$ can be inferred from the set point for the motor flux assuming that $i_m \approx \lambda_{ref}/L_m$ under assumption that this set point is being achieved by the controller.

If the variations of the air-gap fluxes and stator

currents in the rotating frame can be considered negligible, ω_e can be calculated from the value of magnetizing current and supply voltage. In this paper, a simple speed observer will be proposed later.

3.2. PQR transformation

In this chapter a new power transformation algorithm using PQR transformation is presented. The PQR transformation takes the advantages of the PQ and cross vector transformation. The defined instantaneous powers follow power conservation. The three power components are linearly independent of each other.

The average components of the output phase voltage are calculated by (6). In PQR-coordinates, the command voltages are defined as

$$\begin{bmatrix} v_p \\ v_q \\ v_r \end{bmatrix} = \frac{1}{v^s_{0dqs}} \begin{bmatrix} v^s_0 & v^s_{ds} & v^s_{qs} \\ 0 & -\dfrac{v^s_{0dqs}v^s_{qs}}{v^s_{dqs}} & -\dfrac{v^s_{0dqs}v^s_{ds}}{v^s_{dqs}} \\ v^s_{dqs} & -\dfrac{v^s_0 v^s_{qs}}{v^s_{dqs}} & -\dfrac{v^s_0 v^s_{qs}}{v^s_{dqs}} \end{bmatrix} \begin{bmatrix} v^s_0 \\ v^s_{ds} \\ v^s_{qs} \end{bmatrix} = \begin{bmatrix} v^s_{0dqs} \\ 0 \\ 0 \end{bmatrix}, \tag{16}$$

where $v^s_{dqs} = \sqrt{v^{s2}_{ds} + v^{s2}_{qs}}$ and $v^s_{0dqs} = \sqrt{v^{s2}_0 + v^{s2}_{ds} + v^{s2}_{qs}}$.

The output currents in abc-coordinates can be transformed to PQR -coordinates as

$$\begin{bmatrix} i_p \\ i_q \\ i_r \end{bmatrix} = \frac{1}{v^s_{0dqs}} \begin{bmatrix} v^s_0 & v^s_{ds} & v^s_{qs} \\ 0 & -\dfrac{v^s_{0dqs}v^s_{qs}}{v^s_{dqs}} & \dfrac{v^s_{0dqs}v^s_{ds}}{v^s_{dqs}} \\ v^s_{dqs} & -\dfrac{v^s_0 v^s_{qs}}{v^s_{dqs}} & \dfrac{v^s_0 v^s_{qs}}{v^s_{dqs}} \end{bmatrix} \begin{bmatrix} i^s_0 \\ i^s_{ds} \\ i^s_{qs} \end{bmatrix}. \tag{17}$$

Instantaneous real power P is defined as a scalar product of the voltage and current vectors.

$$P = v_p i_p. \tag{18}$$

Instantaneous imaginary powers Q_q and Q_r are defined as a vector product of the voltage and current vectors.

$$Q_q = -v_p i_r,\ Q_r = v_p i_q. \tag{19}$$

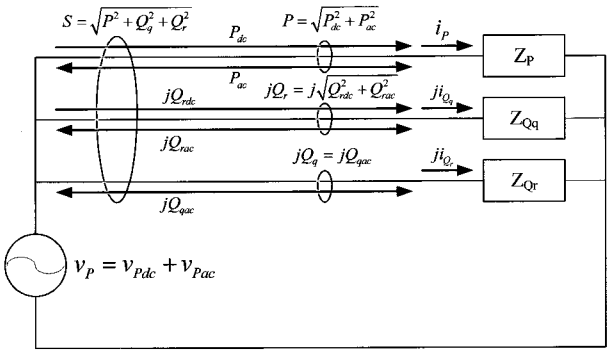

Fig. 5. Power flow in PQR coordinates [12].

It is important to note that the r-axis current i_r contributes to the q-axis instantaneous imaginary power Q_q, and the q-axis current i_q contributes to the r-axis instantaneous imaginary power Q_r. The three powers are linearly independent of each other. Thus, the three current components can be controlled independently by compensating for the three instantaneous powers respectively.

Fig. 5 shows the equivalent circuit diagram and the power flow in PQR coordinates. Three phase source voltages are transformed into one single-phase source voltage v_p that comprises a dc component v_{pdc} and an ac component v_{pac}. The three circuits, completely separated from each other, are just connected in parallel to the source voltage v_p. Thus the three-phase system can now be handled as three single-phase systems. The average power in the p-circuit P_{dc} is the active power and the average power in q-circuit Q_{rdc} is equal to the conventional reactive power. The notation 'j' means the imaginary part that is perpendicular to the p-axis. The other three powers P_{ac}, Q_{rac}, Q_q (Q_{qac}) are useless powers which come from various non-ideal circuit conditions such as unbalanced voltage and loads, distorted system voltages, and non-linear loads [12].

4. DESIGN OF SPEED OBSERVER

In order to build a high-performance speed-sensorless control algorithm for the induction motor drives fed by a matrix converter, more accurate information on the motor speed and more robustness against motor parameters are required. In particular, in the low-speed operation, the machine model-based observer [7,9] does not produce fairly satisfactory performance without a parameter adaptation scheme when motor parameters vary in operation. New observer using the constant flux air-gap and the imaginary power flowing into the motor is proposed to overcome this problem. The proposed speed observer based on the use of the imaginary power would be insensitive to the knowledge of the resistance because the imaginary power is directly

related to flux in the motor and frequency, and not power flow due to the consumption of real power in resistance, The proposed algorithm is also very simple and easy to apply to the real industrial applications.

4.1. Speed observer

The instantaneous real power P is effectively the real power being consumed in the rotor resistance of the motor (R_r/s, s is the slip) ignoring the losses in iron and the stator resistance plus any power stored in the field, and the imaginary powers Q_q and Q_r are related to the instantaneous rate of magnitude change or vector acceleration of the flux vector in the motor. In steady state Q_r becomes equal to the conventional reactive power in a motor [12,13].

Fig. 6 illustrates a vector diagram for an induction motor, showing the relationship between the currents, voltages, and fluxes. The imaginary power is the voltage in one-axis of the motor multiplied by the current in the other axis. The instantaneous imaginary power can be defined.

$$Q_r \approx -i_m \left| v_{emf} \right|. \tag{20}$$

(20) can be rewritten by using (15)

$$Q_r = -L_m i_m^2 (\omega_r + \omega_{sl}), \tag{21}$$

where $\omega_e = \omega_r + \omega_{sl}$.

Given that Q_r can be determined from (19), then (21) can be rewritten so that ω_r is the subject of the expression:

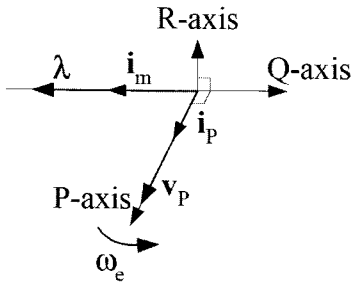

Fig. 6. Approximate vector diagram for an induction motor.

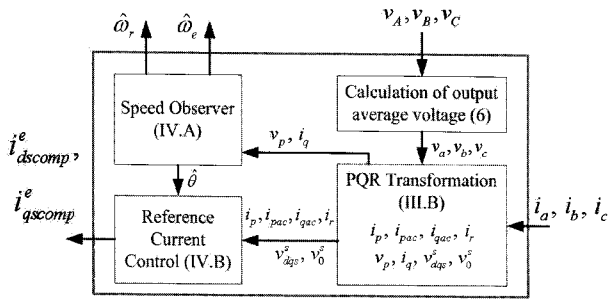

Fig. 7. Speed observer and non-linearity compensation.

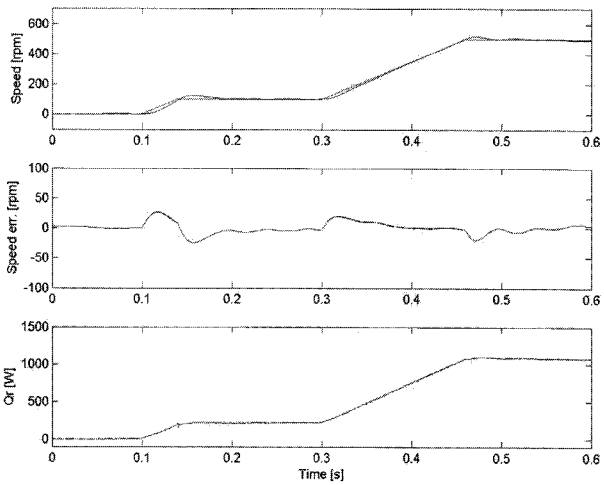

Fig. 8. Speed response of the proposed speed observer: speed reference and speed, speed error, and Qr (Simulation result).

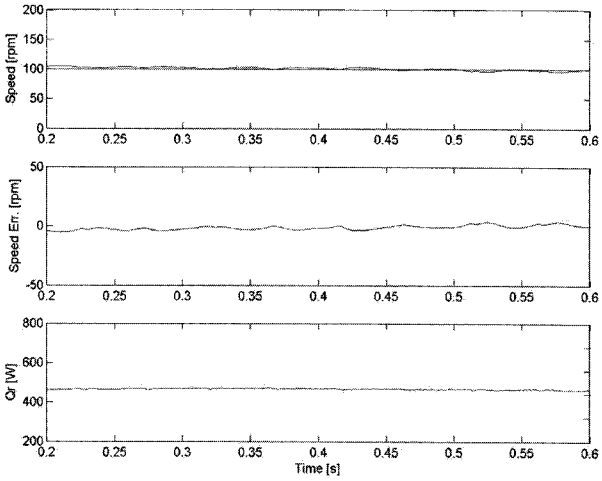

(a)

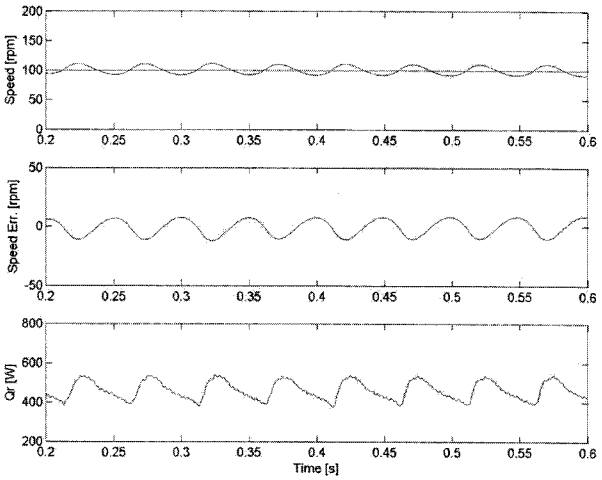

(b)

Fig. 9. Speed response of the proposed sensorless observer in the low speed operation (a) with 0.5 μs commutation delay and (b) with 2 μs commutation delay: speed reference and speed, speed error, and Q_r (simulation result).

$$\omega_r = -\frac{v_p i_q}{L_m i_m^2} - \omega_{sl}, \tag{22}$$

where $\omega_{sl} = i_p / \tau_r i_m$ (see Fig. 6.), $\tau_r = L_r / R_r$, ω_r is the slip frequency, and τ_r is the rotor time constant.

The p-axis voltage v_p and the q-axis current i_q can be calculated by (16) and (17). The proposed scheme is shown in Fig. 7, which consists of a PQR transformation, a speed observer and a reference current control. Fig. 8 shows the simulated waveforms using the ideal matrix converter model for the proposed speed observer. It is shown in Fig. 8 that the estimated speed converges to the actual value by the proposed observer. It can be also seen by this simulation result that the waveform-shape of imaginary power Q_r is almost the same as the estimated speed.

If the matrix converter is no longer considered ideal, the non-linearity of matrix converter can cause considerable distortion in the voltages, especially at low speed [6]. Therefore, the distortion of the Q_r would also occur due to this non-linearity. Fig. 9 shows the speed observer response at the low speed region. From this simulation result, the influence of the non-linearity of the matrix converter on the speed estimation has to be investigated and compensated for these influences.

4.2. Non-linearity modeling for low speed operation

As mentioned in the previous chapter, the non-linearity of matrix converter drives causes the matrix converter output voltage distortion and results in r-axis imaginary power (Q_r) distortion and speed ripple. The voltage disturbances are a function of commutation delays, turn-on and turn-off time of the switching devices, on-state voltage drop and current polarity [6]. However, the commutation delay, on-state voltage drop and the current polarity are varying with the operating conditions. Since it is very difficult to measure the commutation delays and the on-state voltage drop as well as to determine the current sign when the phase currents are closed to zero, it is difficult to compensate for the non-linearities of matrix converter in an off-line manner [8,10]. To alleviate these problems, on-line non-linearity compensation method using PQR transformation is employed to improve speed sensorless performance.

Fig. 10 shows some cases of the three-phase currents in PQR coordinates. In Fig. 10(a) the phase currents are sinusoidal with an ideal matrix converter model. Thus i_r is zero, and i_p and i_q comprise only a dc component. In Fig. 10(b) the phase currents are distorted by the non-linearities of the matrix converter. No zero-sequence component is sensed in the currents, an therefore i_r is zero. The currents i_p and i_q contain an ac component. In Fig. 10(c) the phase current is

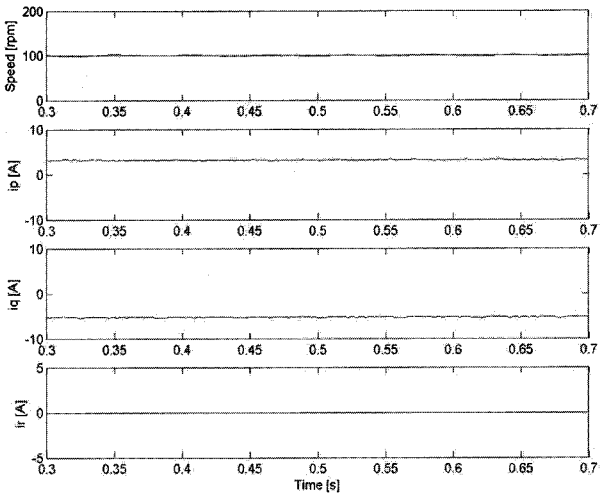

(a)

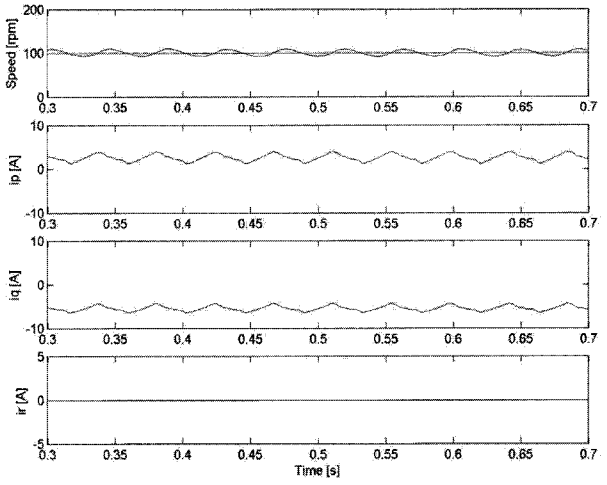

(b)

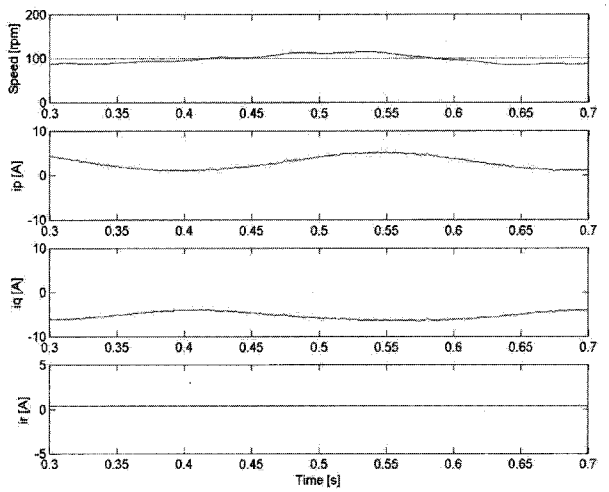

(c)

Fig. 10. Output current representation in PQR coordinates; from top, reference and real speed, p-, q-, and r-axis current (a) with an ideal matrix converter, (b) with a real matrix converter, (c) with an ideal matrix converter and unbalanced current sensing.

sinusoidal but there is an error in the current sensing. Here the sum of the three-phase currents in a-b-c coordinates is not zero. Thus i_r has a nonzero dc-value since it is directly related with the zero sequence component of three-phase currents. The i_p and i_q contain not only a dc component but also an ac component.

If the matrix converter currents are balanced and sinusoidal, the i_p and i_q comprise only the dc component and i_r is zero. When the currents are unbalanced and distorted by the non-linearities of the matrix converter, the unbalanced and harmonic component of the current exists in the i_p, i_q, and i_r. To eliminate these unbalanced and distorted, a reference current control method can be introduced. To make the compensation currents, simple first order high pass filters are used to separate the calculated variables into ac and dc components (Fig. 10). The classified ac and dc components are used to calculate the compensation current for the current controller.

The output phase currents, i_{ds}^s and i_{qs}^s are transformed into PQR coordinates as shown in (17), resulting in i_p, i_q, and i_r. The current i_p consists of an ac component, i_{pac} and a dc component, i_{pdc}. The i_q also consists of an ac component, i_{qac} and a dc component, i_{qdc}. The ac components, i_{pac} and i_{qac} are related with non-linear conditions like harmonics. The i_r represents the zero-sequence component of the output currents. Therefore in order to make the output currents symmetrical and sinusoidal, the current, i_r must be compensated to zero and the current, i_p and i_q have to be controlled to a dc value.

The compensation currents can be represented as

$$i_{pcomp} = i_{pac},\ i_{qcomp} = i_{qac},\ i_{rcomp} = i_r + \frac{v_0^s}{v_{dqs}^s} i_p. \quad (23)$$

The i_{pcomp} is compensated for the p-axis, and the i_{qcomp}, i_{rcomp} are compensated for the q-axis and r-axis, respectively. The compensation currents in PQR coordinates, i_{pcomp}, i_{qcomp}, and i_{rcomp} are inversely transformed to d- and q- axis currents in the stationary reference frame by the inverse transformation of (17).

$$\begin{bmatrix} i_{dcomp} \\ i_{qcomp} \end{bmatrix} = \frac{\sqrt{3/2}}{v_{0dqs}^s} \begin{bmatrix} v_{ds}^s & -\frac{v_{0dqs}^s v_{qs}^s}{v_{dqs}^s} & -\frac{v_0^s v_{ds}^s}{v_{dqs}^s} \\ v_{qs}^s & \frac{v_{0dqs}^s v_{ds}^s}{v_{dqs}^s} & -\frac{v_0^s v_{qs}^s}{v_{dqs}^s} \end{bmatrix} \begin{bmatrix} i_{pcomp} \\ i_{qcomp} \\ i_{rcomp} \end{bmatrix}. \quad (24)$$

The proposed compensation scheme is simple and compensation currents, i_{dscomp}^e and i_{qscomp}^e are calculated instantaneously in the synchronous frame. Each control variable can be controlled independently.

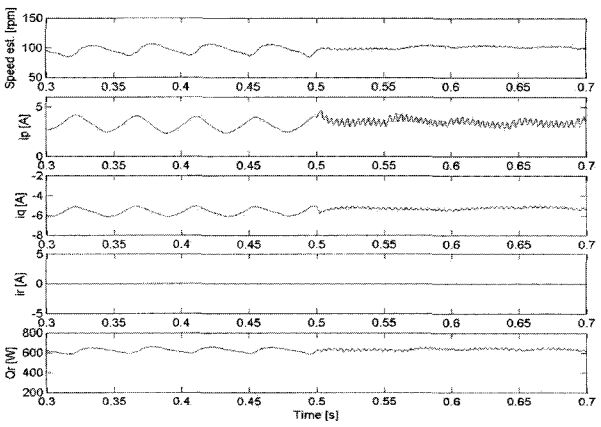

Fig. 11. Simulation results for the presented non-linearity compensation at 100 rpm: Estimated speed, p, q, r-axis current, and Q_r (The compensation starts after 0.5 s).

Fig. 11 shows the simulation waveforms for the non-linearity compensation of the matrix converter drive. Before starting the compensation, the nonlinearity causes undesired speed pulsations of about six times the electrical frequency. The speed estimation error is almost eliminated after starting the compensation.

5. EXPERIMENTS

To confirm the validity of the proposed control algorithm, experiments are carried out. The low speed operation is especially in focus during experiments. The hardware consists of a 3-phase, 380 V, 50 Hz, 4-pole, 3 kW induction motor and power circuit with a matrix converter. The induction motor has the following parameter values: R_s=1.79 Ω, R_r=1.8 Ω, L_s=167 mH, L_r=174.4 mH, and L_m=160 mH. A dual controller system consisting of a 32-bit DSP (ADSP 21062) and a 16-bit microcontroller (80C167), in conjunction with a 12-bit A/D converter board is used to control the matrix converter based induction motor drive. The modulation used a double-sided SVM algorithm with minimized number of commutations and the commutation of the bi-directional switches was performed in a four-step way depending on the output current sign [2].

Figs. 12(a) and 12(b) show the p-, q-, and r-axis currents in the experiments. Fig. 12(c) shows the steady state characteristics of the speed and the phase current at 100 rpm. The nonlinearities cause undesired speed pulsations of about six times the electrical frequency and the p-, q-, and r-axis phase currents are not dc value without nonlinearities compensation as shown in Fig. 12(a).

However, in the proposed compensation scheme, the speed ripple and the distortion in the p-, q-, and r-axis currents waveform are remarkably reduced as

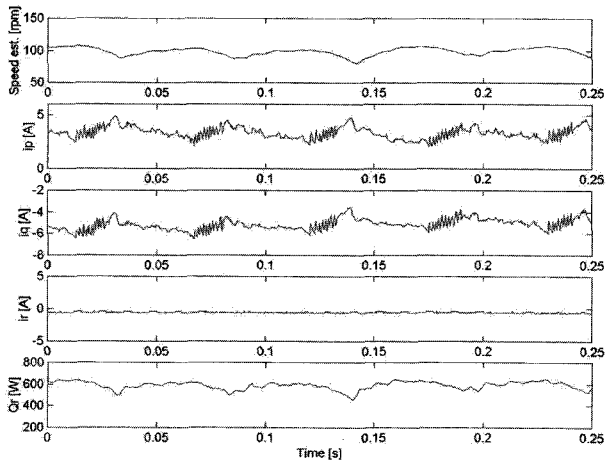

(a)

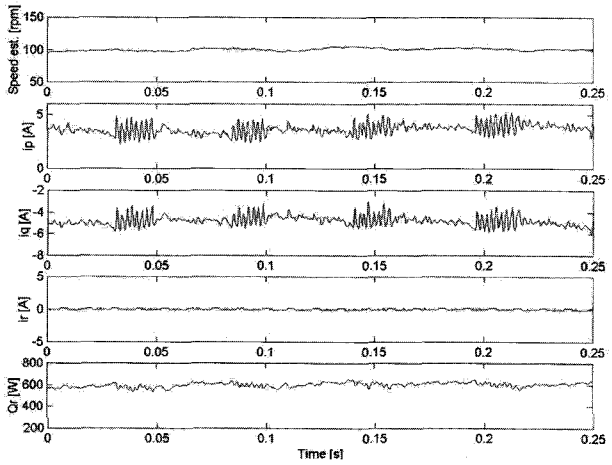

(b)

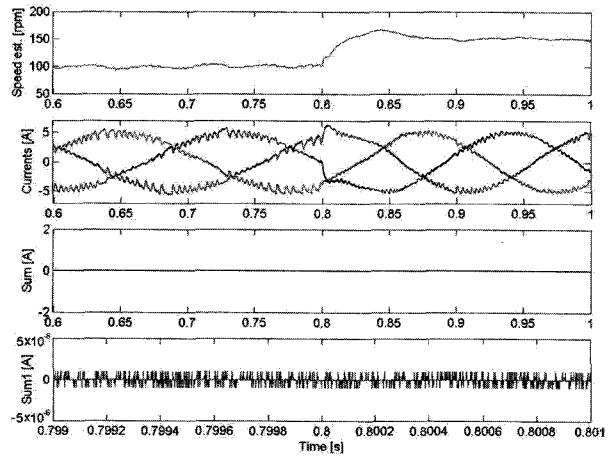

(c)

Fig. 12. Estimated speed and currents in PQR coordinates at the low speed region (a) without non-linearity compensation (estimated speed, p-, q-, r- axis current, and Q_r), (b) with non-linearity compensation (estimated speed, p-, q-, r- axis current, and Q_r), and (c) speed transient response with non-linearity compensation (estimated speed, phase currents, and the sum of three phase currents).

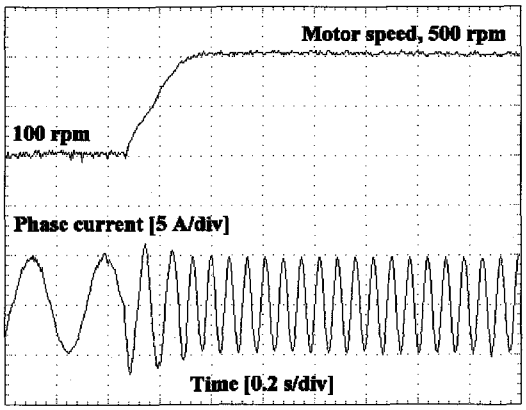

(a) Speed transient from 100 rpm to 500 rpm.

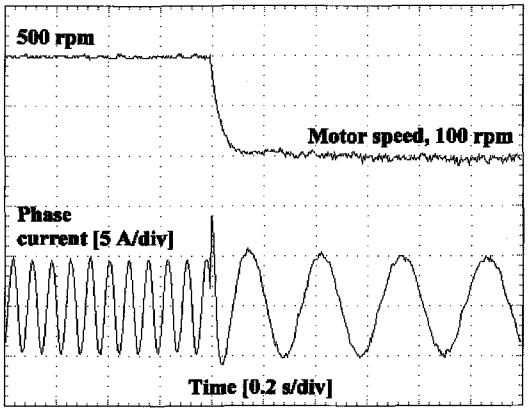

(b) Speed transient from 500 rpm to 100 rpm.

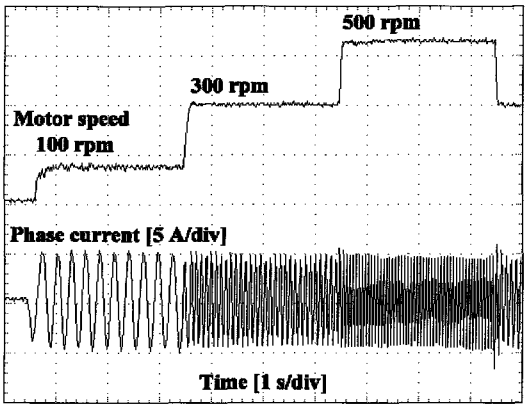

(c) Various speed transient.

Fig. 13. Dynamic response of speed sensorless control with 20% rated road : speed and phase current.

shown in Fig. 12(b). In Fig. 12(c) good speed estimation and a sinusoidal phase current waveform are achieved with speed reference step variation from 100 rpm to 150 rpm. Fig. 13 shows the speed and phase current responses of the proposed sensorless vector control in the various speed references. It is noted here that a very satisfactory dynamic speed response is obtained. Fig. 14 demonstrates the speed dynamic of the proposed sensorless scheme in the

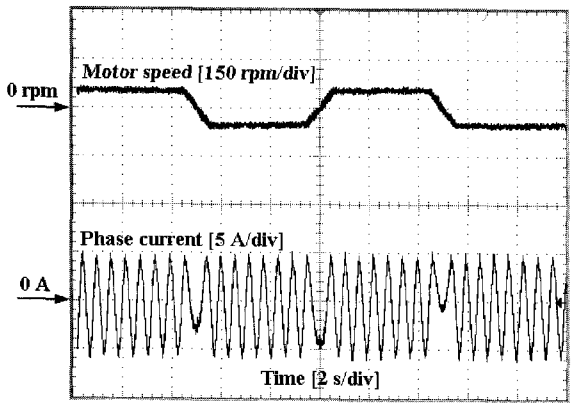

Fig. 14. Dynamic response of speed sensorless control with 20% rated road: speed and phase current (speed transient form 50 rpm to -50 rpm).

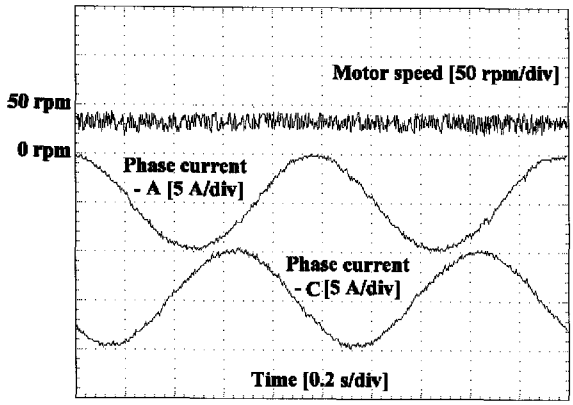

Fig. 15. Speed sensorless control at 30 rpm with 20% rated load: speed and phase currents.

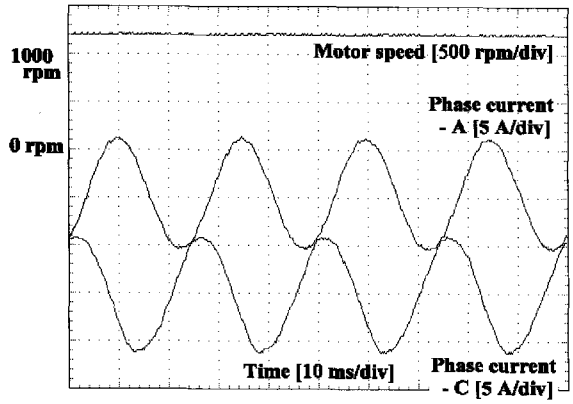

Fig. 16. Speed sensorless control at 1200 rpm with 95% rated load: speed and phase currents.

forward and reverse operation. Fig. 14 shows the speed response for a ramp-speed reference with a slope 150 rpm/s. It is noted here that a smooth and stable zero crossing of the speed is obtained. In Fig. 15, a very good speed estimation and a sinusoidal phase current waveform are achieved at the low speed region down to 30 rpm with 20% rated load. Fig. 16

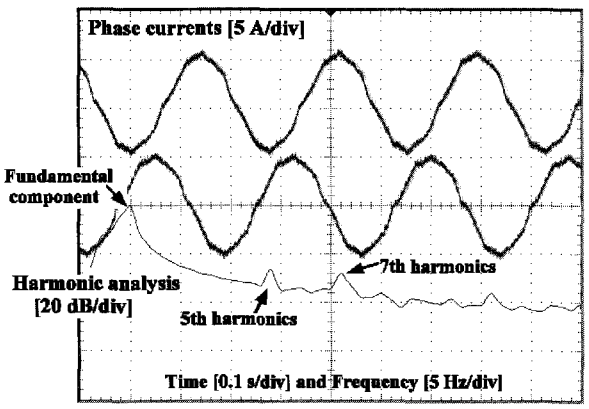

(a)

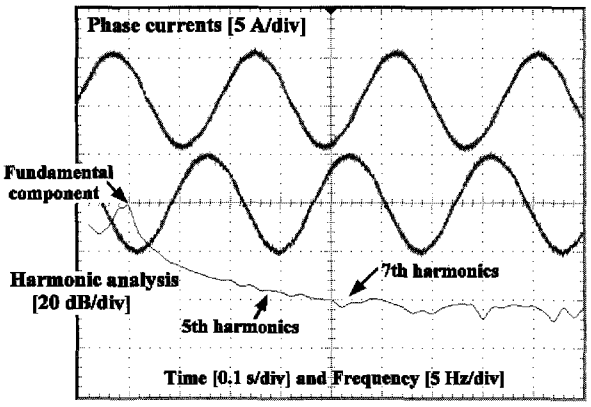

(b)

Fig. 17. Output currents and harmonic analysis (FFT) at 100 rpm with 20% rated load (a) without non-linearity compensation and (b) with non-linearity compensation.

shows the speed estimation performance and phase current at the high-speed region with 100% rated load. Fig. 17 shows the experimental results with and without the proposed compensation method. The motor is also operated at 100 rpm. It can be seen from experimental results that the current pulsations and their 5th and 7th harmonics are reduced with the proposed compensation method using the PQR transformation.

6. CONCLUSIONS

A new and simple sensorless algorithm for induction motor drives fed by matrix converter using the constant air-gap flux and the imaginary power flowing to the motor has been proposed in this paper. The proposed sensorless scheme was independent of the value of the motor parameter. In addition, a non-linearity compensation strategy using PQR transformation has been employed to make better the speed control performance in the low speed region. The experimental results have shown that the satisfactory speed sensorless performance in the various speed operation has been obtained.

REFERENCES

[1] M. P. Kazmierkowski, R. Krishnan, and F. Blaabjerg, *Control in Power Electronics - Selected Problems*, Chapter 3, Academic Press, 2002.

[2] P. Nielsen, F. Blaabjerg, and J. K. Pedersen, "New protection issues of a matrix converter: Design considerations for adjustable-speed drives," *IEEE Trans. on Industry Applications*, vol. 35, no. 5, pp. 1150-1161, Sept./Oct. 1999.

[3] P. W. Wheeler, J. Rodriguez, J. C. Clare, L. Empringham, and A. Weinstein, "Matrix converter: A technology review," *IEEE Trans. on Industrial Electronics*, vol. 49, no. 2, pp. 276-288, April 2002.

[4] L. Huber and D. Borojevic, "Space vector modulated three-phase to three-phase matrix converter with input power correction," *IEEE Trans. on Industry Applications*, vol. 31, no. 6, pp. 1234-1246, Nov./Dec. 1995.

[5] C. Klumpner, P. Niesen, I. Boldea, and F. Blaabjerg, "A new matrix converter-motor (MCM) for industry applications," *IEEE Trans. on Industrial Electronics*, vol. 49, no. 2, pp. 325-335, April 2002.

[6] K. B. Lee and F. Blaabjerg, "A nonlinearity compensation method for a matrix converter drive," *IEEE Power Electronics Letters*, vol. 3, no. 1, pp. 19-23, 2005.

[7] K. B. Lee and F. Blaabjerg, "Reduced order extended Luenberger observer based sensorless vector control driven by matrix converter with non-linearity compensation," *IEEE Trans. on Industrial Electronics*, vol. 53, no. 1, pp. 66-75, Feb. 2006.

[8] K. B. Lee and F. Blaabjerg, "Performance improvement of sensorless vector control for matrix converter drives using PQR power theory," *Electrical Engineering*, vol. 89, no. 8, pp. 607-616, Sept. 2007.

[9] J. Holtz, "Sensorless control of induction motor drives," *Proc. of the IEEE*, vol. 90, no. 8, pp. 1359-1394, Aug. 2002.

[10] N. Urasaki, T. senjyu, K. Uezato, and T. Funabashi, "A dead-time compensation strategy for permanent magnet synchronous motor drive suppressing current distortion," *Proc. of IEEE IECON03*, pp. 1255-1260, 2003.

[11] D. W. Novotny and T. A. Lipo, *Vector Control and Dynamics of AC Drives*, Oxford University Press, 1997.

[12] H. Kim, F. Blaabjerg, and B. Bak-Jensen, "Spectral analysis of instantaneous powers in single-phase and three-phase systems with use of p-q-r theory," *IEEE Trans. Power Electronics*, vol. 17, no. 5, pp. 711-720, Sept. 2002.

[13] R. E. Betz and T. Summers, "Speed estimation for induction machines using imaginary power," *Proc. of IAS03*, pp. 117-123, 2003.

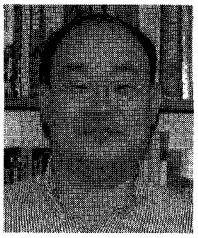

Kyo-Beum Lee received the B.S. and M.S. degrees in Electrical and Electronic Engineering from Ajou University, Suwon, Korea, in 1997 and 1999, respectively. He received the Ph.D. degree in Electrical Engineering from Korea University, Seoul, Korea in 2003. From 2003 to 2006, he was with the Institute of Energy Technology, Aalborg University, Aalborg, Denmark. From 2006 to 2007, he was with the Division of Electronics and Information Engineering, Chonbuk National University, Jeonju, Korea. Since 2007 he has been with the School of Electrical and Computer Engineering, Ajou University, Suwon, Korea. He has received two IEEE prize paper awards. His research interests include electric machine drives and power electronics.

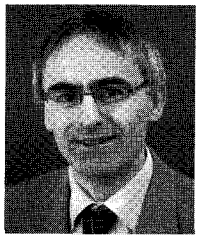

Frede Blaabjerg received the M.Sc.EE. from Aalborg University, Denmark in 1987, and the Ph.D. degree from the Institute of Energy Technology, Aalborg University, in 1995. He was employed at ABB-Scandia, Randers, from 1987-1988. During 1988-1992 he was a Ph.D. student at Aalborg University. He became an Assistant Professor in 1992 at Aalborg University, in 1996 Associate Professor and in 1998 Full Professor in Power Electronics and Drives the same place. In 2006 he became the Dean of Faculty of Engineering and Science at Aalborg University. His research areas are in power electronics, static power converters, ac drives, switched reluctance drives, modeling, characterization of power semiconductor devices and simulation, wind turbines and green power inverter. He is the author or co-author of more than 300 publications in his research fields including the book 'Control in Power Electronics' (Eds. M.P. Kazmierkowski, R. Krishnan, F. Blaabjerg) 2002, Academic Press. During the last years he has held a number of chairman positions in research policy and research funding bodies in Denmark. He is Associated Editor of the IEEE Transactions on Industry Applications, IEEE Transactions on Power Electronics, Journal of Power Electronics and of the Danish journal Elteknik and in 2006 he became Editor-in-Chief of IEEE Transactions on Power Electronics. He received the 1995 Angelos Award for his contribution in modulation technique and control of electric drives, and an Annual Teacher prize at Aalborg University, also 1995. In 1998 he received the Outstanding Young Power Electronics Engineer Award from the IEEE Power Electronics Society. He has received five IEEE Prize paper awards during the last six years. He received the C.Y. O'Connor fellowship 2002 from Perth, Australia, the Statoil-prize in 2003 for his contributions in power electronics and the Grundfos-prize in 2004 for his contributions in power electronics and drives.